Stretto di Messina

Concessionaria per la progettazione, realizzazione e gestione del collegamento stabile tra la Sicilia e il Continente Organismo di Diritto Pubblico
(Legge n° 1158 del 17 dicembre 1971, modificata dal D.Lgs. n°114 del 24 aprile 2003)

Eurolink

PONTE SULLO STRETTO DI MESSINA

PROGETTO DEFINITIVO

EUROLINK S.C.p.A.

IMPREGILO S.p.A. (MANDATARIA)
SOCIETÀ ITALIANA PER CONDOTTE D'ACQUA S.p.A. (MANDANTE)
COOPERATIVA MURATORI E CEMENTISTI - C.M.C. DI RAVENNA SOC. COOP. A.R.L. (MANDANTE)
SACYR S.A.U. (MANDANTE)
ISHIKAWAJIMA - HARIMA HEAVY INDUSTRIES CO. LTD (MANDANTE)
A.C.I. S.C.P.A. - CONSORZIO STABILE (MANDANTE)

IL PROGETTISTA	IL CONTRAENTE GENERALE	STRETTO DI MESSINA	STRETTO DI MESSINA
Ing E.M.Veje COWI Eurolink Dott. Ing. E. Pagani Ordine Ingegneri Milano n° 15408	Project Manager (Ing. P.P. Marcheselli)	Direttore Generale e RUP Validazione (Ing. G. Fiammenghi)	Amministratore Delegato (Dott. P. Ciucci)

PS0279_F0

Unità Funzionale	OPERA DI ATTRAVERSAMENTO
Tipo di sistema	METODI E SISTEMI TEMPORANEI PER LA CONSTRUZIONE E IL MONTAGGIO
Raggruppamento di opere/attività	SOVRASTRUTTURE
Opera - tratto d'opera - parte d'opera	IMPALCATO
Titolo del documento	VERIFICA STRUTTURALE DELLE FASI DI MONTAGGIO

CODICE: C G 1 0 0 0 | P | C L | D | P | M T | S 5 | I M | 0 0 | 0 0 | 0 0 | 0 1 | F0

REV	DATA	DESCRIZIONE	REDATTO	VERIFICATO	APPROVATO
F0	20-06-2011	EMISSIONE FINALE	LTS/OVS/SOLA	LTS/LSJ	LSJ

NOME DEL FILE: PS0279_F0.docx

INDICE

1 Introduction

COWI has been asked to review the construction methods for the suspended deck as proposed by Eurolink/Cimolai with the purpose of verifying the permanent structures.

The proposed construction methods are reviewed in order to verify the feasibility and to evaluate the global and local impact on the designed structures in order to determine the requirement for additional reinforcement of the structures.

1.1 Scope of general review

The review of the deck construction methods tower is based on the information provided by Cimolai. The Cimolai reports and drawings reviewed as part of this task are listed in Table 1-1 and Table 1-2.

Table 1-1 Cimolai reports reviewed

Report Title	Document No.
Roadway segments during assembly phases	2002159RCD0037 0
Metodo do Montaggio Impalcato	2002159-CIM-EMS-0500 0

Table 1-2 Cimolai drawings reviewed

Drawing Title	Document No.
Impalcato - Fasi di montaggio - Montaggio di un element modulare tipico - Vista in alzato	2002159D000250A
Impalcato - Fasi di montaggio - Montaggio di un element modulare tipico - Pianta e sezione traversale	2002159D000251B
Carpentaria impalcato - Attrezzature di montaggio - Dispositivo di sollevamento - Tavola 1 di 2	2002159D000252B
Carpentaria impalcato - Attrezzature di montaggio - Dispositivo di sollevamento - Tavola 2 di 2	2002159D000253B
Traliccio per trasporto bozzelli di sollevamento conci di impalcato	2002159D0002540
Assieme generale - Pianta e prospetto	2002159D0002100
Suddivisione conci impalcato (Lato Calabria) - Pianta e prospetto	2002159D0002110

Suddivisione conci impalcato (Lato Sicilia) - Pianta e prospetto	2002159D0002120
Montaggio impalcato - Montaggio conci 1 a 2S, 2C, 3S, 3C	2002159D0002130
Montaggio impalcato - Montaggio conci 4S, 4C, 5S, 5C	2002159D0002140
Montaggio impalcato - Montaggio conci 6S, 6C, 7S, 7C	2002159D0002150
Montaggio impalcato - Montaggio conci 8S, 8C, 9S, 9C	2002159D0002160
Montaggio impalcato - Montaggio conci 10S, 10C, 11S, 11C	2002159D0002170
Montaggio impalcato - Montaggio conci 12S, 12C, 13S, 13C	2002159D0002180
Montaggio impalcato - Montaggio conci 14S, 14C, 15S, 15C	2002159D0002190
Montaggio impalcato - Montaggio conci 16S, 16C, 17S, 17C	2002159D0002200
Montaggio impalcato - Montaggio conci 18S, 18C, 19S, 19C	2002159D0002210
Montaggio impalcato - Montaggio conci 20S, 20C, 21S, 21C	2002159D0002220
Montaggio impalcato - Montaggio conci 22S, 22C, 23S, 23C	2002159D0002230
Montaggio impalcato - Montaggio conci 24S, 24C, 25S, 25C	2002159D0002240
Montaggio impalcato - Montaggio conci 26S, 26C	2002159D0002250
Montaggio impalcato - Montaggio concio 35C - Sottofasi a, b, c	2002159D0002260
Montaggio impalcato - Montaggio concio 35C - Sottofasi d, e, f	2002159D0002270
Montaggio impalcato - Montaggio concio 35C - Sottofasi g, h, i	2002159D0002280
Montaggio impalcato - Montaggio concio 34C - Sottofasi a, b, c	2002159D0002290
Montaggio impalcato - Montaggio concio 34C - Sottofasi d, e, f	2002159D0002300
Montaggio impalcato - Montaggio concio 34C - Sottofasi g, h, i	2002159D0002310
Montaggio impalcato - Montaggio conci 32C a 33C	2002159D0002320
Montaggio impalcato - Montaggio concio 31C - Sottofasi a, b, c	2002159D0002330

Montaggio impalcato - Montaggio concio 31C - Sottofasi d,e,f	2002159D0002340
Montaggio impalcato - Montaggio concio 31C - Sottofasi g, h, i	2002159D0002350
Montaggio impalcato - Montaggio conci 29C a 30C	2002159D0002360
Montaggio impalcato - Montaggio concio 28C - Sottofasi a, b, c	2002159D0002370
Montaggio impalcato - Montaggio concio 28C - Sottofasi d, e - Montaggio concio 27C	2002159D0002380
Fasi di montaggio impalcato - Montaggio conci 1 a 25 - Sottofase 1	2002159D0002600
Fasi di montaggio impalcato - Montaggio conci 1 a 25 - Sottofase 2	2002159D0002610
Fasi di montaggio impalcato - Montaggio conci 1 a 25 - Sottofase 3	2002159D0002620
Fasi di montaggio impalcato - Montaggio conci 1 a 25 - Sottofase 4	2002159D0002630
Fasi di montaggio impalcato - Montaggio conci 1 a 25 - Sottofase 5	2002159D0002640
Fasi di montaggio impalcato - Montaggio conci 1 a 25 - Sottofase 6	2002159D0002650
Fasi di montaggio impalcato - Montaggio conci 1 a 25 - Sottofase 7	2002159D0002660
Fasi di montaggio impalcato - Montaggio concio 2C - Sottofasi 8, 9, 19	2002159D0002670
Fasi di montaggio impalcato - Montaggio conci 3S e 3C - Sottofasi 11, 12, 13	2002159D0002680
Fasi di montaggio impalcato - Montaggio conci 3S e 3C - Sottofasi 14 e 15	2002159D0002690
Montaggio impalcato - Systemazione aree di stocaggio conci di impalcato	2002159D0006500
Movimantazione dei conci di impalcato	2002159D0006510
Impalcato - Montaggio - Dettaglio attacco pendino	2002159D0002550

In cases where information was not available, reasonable assumptions were made as described in the relevant sections. The construction method review is primarily focused on verification of the permanent deck structure for the construction loads and includes the following scope:

- General comments and observations regarding the proposed construction method;

- Assessment of the aerodynamic stability of the erected deck during construction. Erection stages comprising approximately 5%, 10%, 15%, 20%, 25%, 50% and 100% of the deck has been investigated;
- Assessment of deflections and stresses in the cantilevered part of a typical deck section during erection in order to verify the geometry at the connection to adjacent deck sections;
- Review of the proposed connection detail between the deck section and the lifting systems in order to verify the present design and to evaluate if reinforcement and/or redesign of the deck structure will be required;
- Assessment of the local load effects on the deck structure introduced by the extension truss proposed for the lifting of deck sections and evaluation if reinforcement and/or redesign of the deck structure will be required;
- Assessment of local load effects in the deck introduced by the erection of deck sections near the tower and in the side span and evaluation if reinforcement and/or redesign of the deck structure will be required;
- Assessment of load effects during storage and sea transportation of deck sections.

The extent of the analysis and design calculations are intended to provided a general indication of the feasibility of the construction methods and expected modifications to the permanent deck structure. The results presented are based on the expected loadings at the critical cross sections. A more comprehensive detailed analysis of all construction stages and loadings may result in some optimizations.

2 General review

A general review of the various methods proposed by Cimolai has been made based upon experience from similar processes. No check of Cimolai's calculations has been made.

2.1 General handling of elements

Fabrication and erection of major bridges is a mass production and repetitive handling of similar elements. The handling starts with plates and profiles, then panels and subassemblies and finally erection elements.

The handling including sea fastening should preferably be made without welded attachments. It is our experience that repetitive use of non welded handling appliances is cost effective and leaves less repairs on the permanent structures. At the same time it is also faster to fasten and unfasten the elements during operations often on the critical path.

2.2 Sea transport

Slamming by the waves on the bridge elements during sea transport should be avoided. Possible slamming would increase the loads on the elements considerably and would probably be able to damage the relatively thin walled panels.

Sea water should also be prevented to enter into the internal parts of the bridge elements, because salt deposits are not acceptable and cleaning is difficult in practice.

3 General comments to proposed construction method

The girder erection is in general done with winches on the bridge deck. The hoists are attached to the permanent hangers for the girder section.

When the correct level has been reached the permanent pin bolts are installed for the hanger sockets and the load is transferred to the hanger/deck connection.

Temporary steel truss structures are provided in order to obtain access to the hangers for attachment of the hoists and hydraulic devices for adjustment of the hanger position relative to the bridge deck are installed on the steel truss.

In the following our comments to the erection concept are given.

1 The first lift of the central sections (section no. 2s and no.1) with the lifting girder on top is the heaviest lift. The lifting machinery is located on the girder to be lifted and is operated by remote control.

2 A number of hangers around the middle of the main span are equipped with spherical bearings that can take rotations in two directions. Such bearings have a very tight tolerance to the pin. (g6 ISO 286). The fitting of the pin on site with full load on the hanger is considered to be very difficult as a very accurate alignment needs to be obtained.

3 The long hangers are attached with a normal hanger connection where the tolerance between the pin and the socket is of about 0.2 mm. Even with this tolerance fitting of the connection is considered to be very difficult with full load on the hangers.

4 Trial fitting between all erection girder elements is assumed before erection. During trial fitting erection attachments are welded on the mating elements so that they can easily be brought into the correct relative position during erection by connecting the erection attachments. Connecting the erection attachments between the mating sections seems not to be addressed. The fit up will also be influenced by the presence of the erection girder standing on the tip of the previously erected girder. This situation is not present during trial assembly and should be considered when determining the position of erection attachments. For connection of the brackets it might be necessary to lift the girder to a higher level temporarily.

5 As the deck section hoists are attached to the permanent hanger ropes the risk of damaging the hanger ropes during installation and removal of the hoists shall be considered. The hoist arrangement is seated on the ends of the sockets of the hanger rope and adequate care shall be taken not to damage the HDPE sheathing or the thermal shrinkage sleeve at the end of the socket.

4 Aerodynamic stability during erection

This section contains an analysis of the aerodynamic stability of the main span during erection.

4.1 Summary of aerodynamic stability during erection

Table 4-1 contains an overview of the calculated critical wind speeds, *U*. The phase number refers to the IBDAS calculations and *L* is the total length of the girders in the main span. Phase 1100 is the full bridge but still without screens and railings.

Table 4-1 Critical wind speeds, U, for selected construction stages

Phase	L [m]	U [m/s]
210	150	67.7
230	390	61.5
240	510	52.6
250	630	50.7
270	870	47.2
340	1710	41.9
400	2430	40.0 (67)
1100	*3300*	*46.0*

(…) Indicates the critical wind speed with wind screens according to what stated in CRA Construction Risk Analysis Report CG1000-P-SR-D-P-GE-R5-00-00-00-00-10_C

Wind screens will be erected at a certain phase of deck construction in order to maintain stability under the assumed ULS wind speed (i.e. 54m/s).

4.2 Approach

The approach is described below.

- An eigenvalue analysis of the construction stages has been performed by use of IBDAS model version 3.3d. The IBDAS model has been used to identify vertical and torsion mode shapes, eigen frequencies and generalised mass contributions.

- The aerodynamic derivatives for the girder cross section for construction are obtained from the wind tunnel section model testing of the construction stage at FORCE, /2/. Parallel tests carried out at BLWTL yields the same results but they do not cover as large a range of wind speeds, hence the FORCE data were used.

- The above structural and aerodynamic values have been combined in an AMC flutter analysis to determine the aerodynamic stability for a construction stage for a given combination of vertical and torsion mode shapes. The differences in mode shapes have been taken into account by use of modal correction coefficients using the method outlined in /1/.

4.3 Critical wind speeds

Table 4-2 contains the mode shapes and eigenfrequencies used in the flutter calculations. Furthermore, the table contains critical wind speeds, *U*, found for the investigated combinations of vertical and torsion mode shapes.

Table 4-2 Mode shapes and critical wind speeds, U

Mode	**Mode shapes**	**Freq. [Hz]**	**Modes**	***U* [m/s]**
Phase 210, *L* = 150 m				
3 Vertical assymmetrical		0.063	3 + 10 9 + 10	> 100 67.7
9 Vertical symmetrical	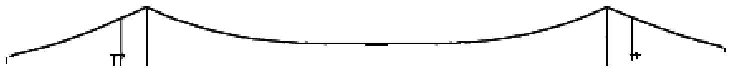	0.081	3 + 18 9 + 18	> 100 > 100
10 Torsion symmetrical	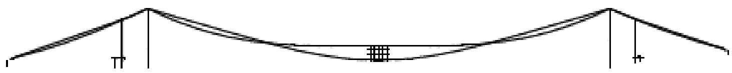	0.087		
18 Torsion symmetrical		0.113		
Phase 230, *L* = 390 m				
3 Vertical asymmetrical		0.064	3 + 10 9 + 10	> 100 63.5
9 Vertical symmetrical		0.080	3 + 11 9 + 11	> 100 61.5
10 Torsion symmetrical		0.088		
11 Torsion symmetrical		0.088		

Mode	**Mode shapes**	**Freq. [Hz]**	**Modes**	***U* [m/s]**
	Phase 240, *L* = 510 m			
3 Vertical asymmetrical		0.064	3 + 7 9 + 11	52.6 60.0
7 Torsion asymmetrical		0.068		
9 Vertical symmetrical		0.079		
11 Torsion symmetrical	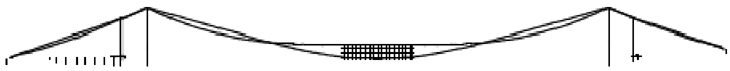	0.089		
	Phase 250, *L* = 630 m			
3 Vertical asymmetrical		0.065	3 + 7 3 + 11 9 + 11	50.7 > 100 60.7
7 Torsion asymmetrical		0.069		
9 Vertical symmetrical		0.079		
11 Torsion symmetrical	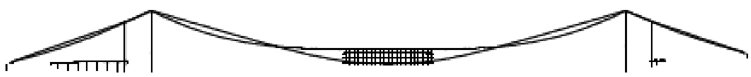	0.090		

Mode	**Mode shapes**	**Freq. [Hz]**	**Modes**	***U* [m/s]**
	Phase 270, *L* = 870 m			
3 Vertical asymmetrical	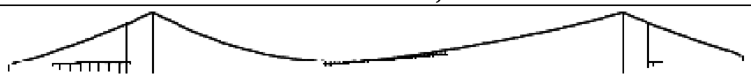	0.064	3 + 7 9 + 12	47.2 59.2
7 Torsion asymmetrical		0.070		
9 Vertical symmetrical		0.079		
12 Torsion symmetrical		0.092		
	Phase 340, *L* = 1710 m			
3 Vertical asymmetrical		0.059	3 + 7 9 + 14	41.9 58.1
7 Torsion asymmetrical		0.072		
9 Vertical symmetrical	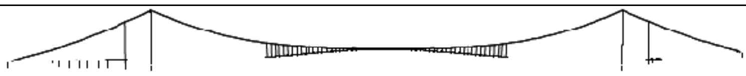	0.080		
14 Torsion symmetrical	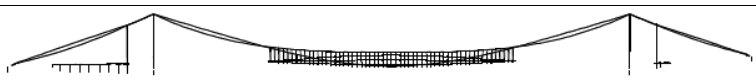	0.098		

Mode	**Mode shapes**	**Freq. [Hz]**	**Modes**	***U* [m/s]**
	Phase 400, *L* = 2430 m			
4 Vertical asymmetrical		0.057	4 + 5 10 +15	40.0 57.2
5 Torsion asymmetrical		0.072		
10 Vertical symmetrical		0.079		
15 Torsion symmetrical		0.098		
	Phase 1100, *L* = 3300 m			
3 Vertical asymmetrical		0.065	3 + 8	46.0
8 Torsion asymmetrical		0.081		

In Figure 4-1 critical wind speeds, *U*, are illustrated as a function of the total length of the girders in the main span, *L*.

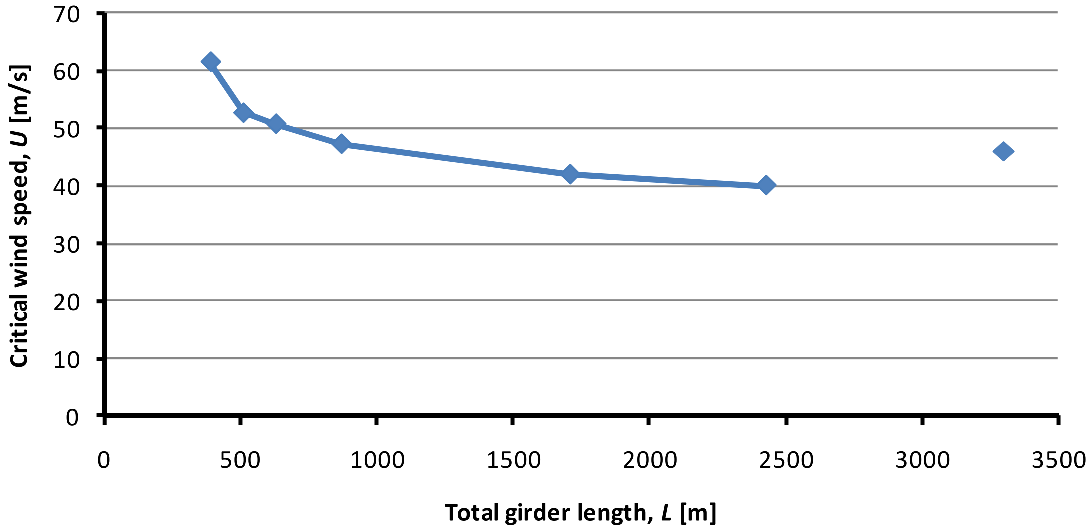

Figure 4-1 Critical wind speeds for selected construction stages

5 Cantilevered part of a typical erection section

To get an estimate of the vertical deflection of the typical erection section, the local beam model shown in Figure 5-1 is developed. As shown in Figure 5-1 the model is supported in vertical direction in the four hanger anchorages.

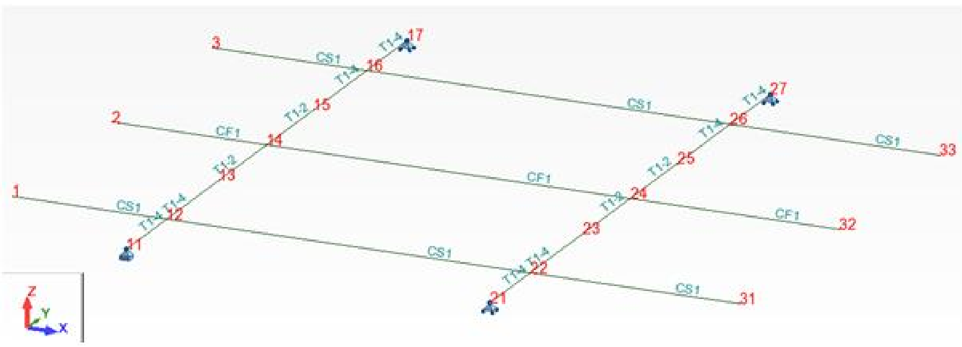

Figure 5-1 Local beam model of the 60m erection section

Section properties for the beam elements shown in Figure 5-1 are determined in ADVERS. The section properties for the roadway girder are taken as type CS1 and railway as type CF1. The cross girder has a varying cross section within this erection segment, whereas the section properties are taken as an approximation to the girder geometry. Figure 5-2 is showing the position of the section properties in section 2 which is representing the cross girder in the beam model from centre bridge to the kink in the bottom plate and section 4 is representing the cross girder from the kink to the hanger anchorage.

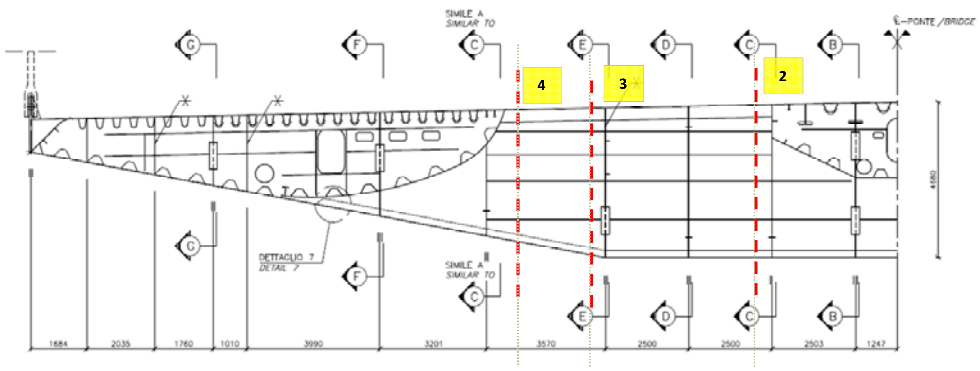

Figure 5-2 Positions for section properties in cross girder

Cross section properties for the various beam elements calculated in ADVERS are shown in Table 5-1.

Table 5-1 Section properties for beam elements in local model

Beam element	As [m^2]	Iy [m^4]	Iz [m^4]	J [m^4]
T1 section 2	0.335	1.265	0.686	1.121
T1 section 4	0.343	0.926	0.732	1.086
CS1	0.568	0.405	9.319	0.967
CF1	0.389	0.316	2.163	0.642

The segment is loaded with dead load with a characteristic steel density set to 77kN/m^3 and an additional estimated superimposed dead load of 10% for service lane, rail fastening, base plates etc. The characteristic deflection of the general erection segment is shown in Figure 5-3.

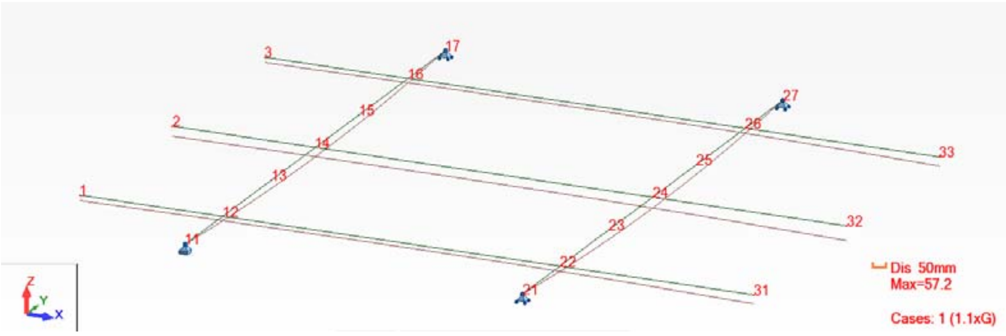

Figure 5-3 Supports, nodes and deflection plot for the local beam model

As shown in Figure 5-3 the maximum deflection is 57mm for the longest cantilevered part of the railway girder. The deformations for the rest of the points are shown in Table 5-2.

Table 5-2 Nodal displacement for the local beam model

Node	1	2	3	11	12	13	14	15	16	17	21	22	23	24	25	26	27	31	32	33
-Uz [mm]	21	39	21	0	17	32	36	32	17	0	0	20	37	42	37	20	0	35	57	35

The deformation of the girder segment during erection needs to be accounted for in order to fit the segment to the final geometry after erection. Cimolai has an idea of counter balancing the cantilevered part of deflections by introducing a temporary support beam. This method needs to be explained in further detail and reviewed.

Due to the cantilevered parts stresses due to dead load deflections may be "locked into" the structure during installation. For the roadway girder it is estimated that these stresses locally can reach a maximum of 55MPa, see the figure below. For the railway girder the stresses are assumed to be less due to the lesser dead load and a symmetrical cross section.

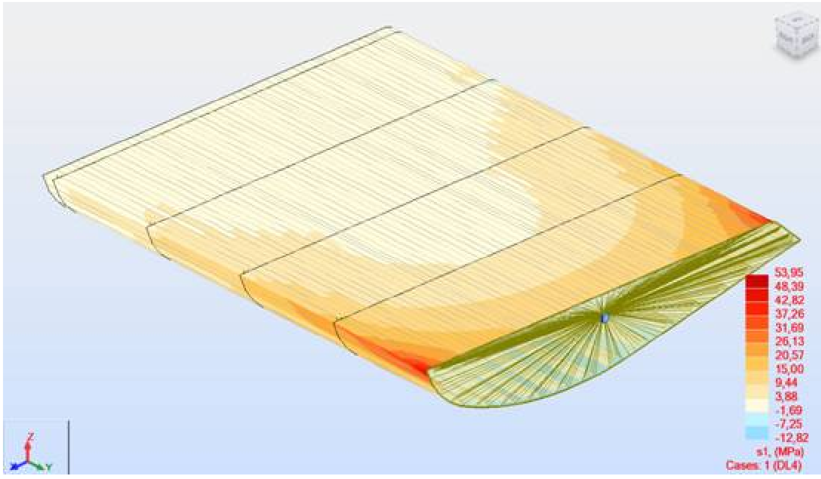

Figure 5-4 Roadway girder, stresses due to dead load deflections

It should be noted that in the calculation the weight of surfacing, installations ect. has not been accounted for, since not present during erection. However this should be accounted for when considering the calculations for pre-camber.

6 Connection detail - deck and sheave block at bottom

An elevation and section of the proposed solution is shown in Figure 6-1.

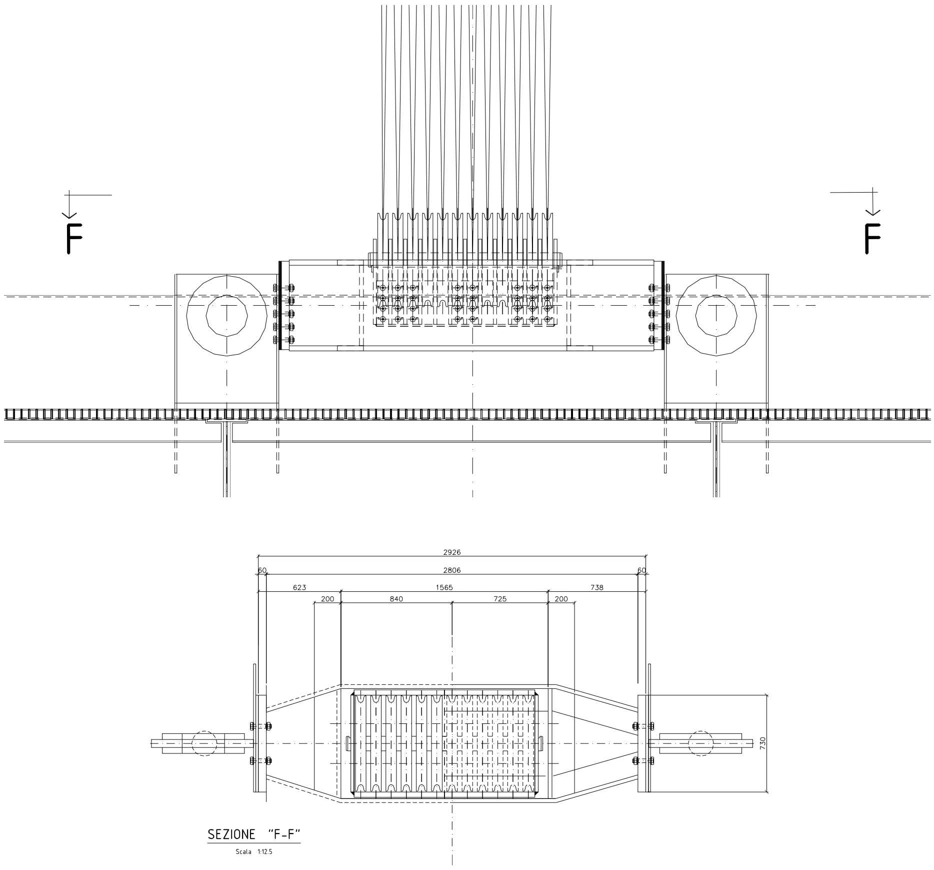

Figure 6-1 Proposed solution of the connection detail of the sheave block and the hanger anchorage

The only steel in the existing design that is available for the bolted connection is shown in red in Figure 6-2.

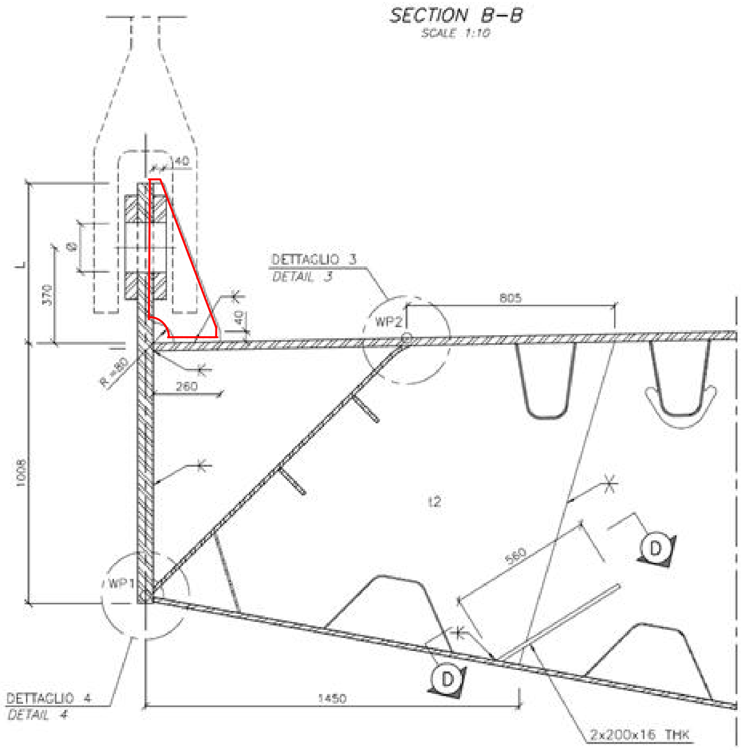

Figure 6-2 Section at the hanger anchorage showing the available steel for the bolted connection detail

Alternative 1: Use the pinholes for the hanger replacement for the attachment of the sheave block as shown in Figure 6-3.

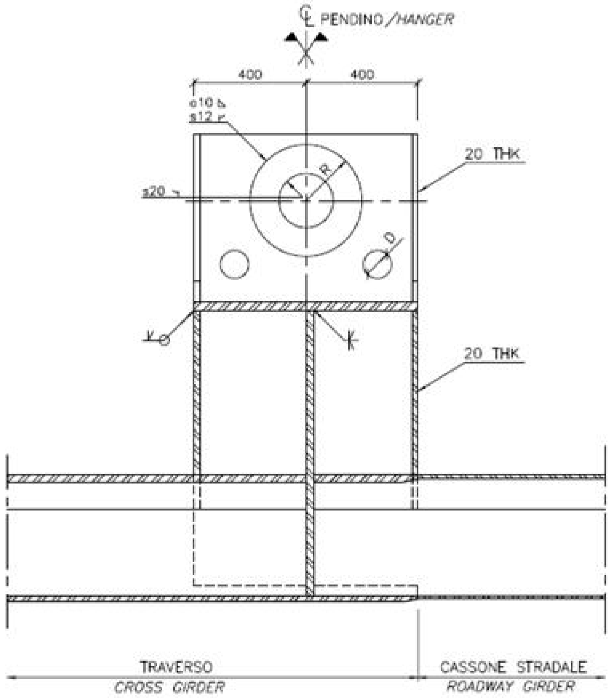

Figure 6-3 Pinholes in hanger anchorage for hanger replacement, shown as "D"

Alternative 2: Enlarge the thickness and extend the side plate in the hanger anchorage. Further more add a temporary plate for the erection situation as shown in Figure 6-4.

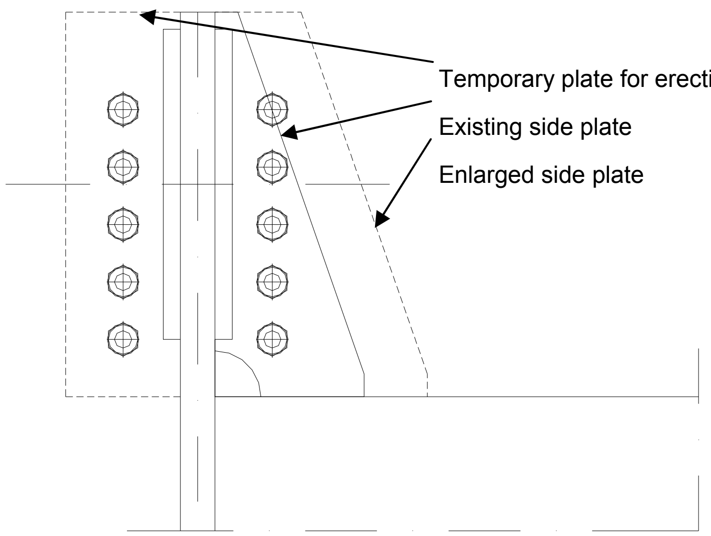

Figure 6-4 Enlarged side plate and temporary plate for the erection situation

The general payload is taken for a general 60m erection segment at the main span. The weight of the 60m segment with a combination of roadway girder 1 (CS1), railway girder 1 (CF1) cross girder 1 (T1) and hanger anchorage 1 (AP1) is shown in Table 6-1.

Table 6-1 Weight of a general 60m erection segment

Element	**Dead load [kN/m]**	**Nos. / Length [m]**	**Total [kN]**
Cross girder	1580	2	3160
Roadway girder	41.8	105	4389
Railway girder	27.7	52.5	1454
Hanger anchorage	24.1	8	193
Service lane, base plates and additional weight under transportation.			945
Grand Total			10141

As shown in Table 6-1 the total weight of a segment in the main span is 10141kN. With eight hanger anchorages per erection section and an estimated dynamic factor of 1.10, 1.25 for skewing effect for a lift with four lifting points, a safety factor of 1.35 the design reaction from the sheave block is:

$$R_{\text{sheave block,d}} = \frac{10141 \cdot 1.1 \cdot 1.25 \cdot 1.35}{8} = 2353\text{kN}$$

The bending moment in the bolted connection is assumed to be zero, whereas the reaction from the sheave block is acting with an eccentricity compared with the regular hanger force. The reaction is therefore applied to the local FE-model of the hanger anchorage in the centre line of the connection as shown in Figure 6-5.

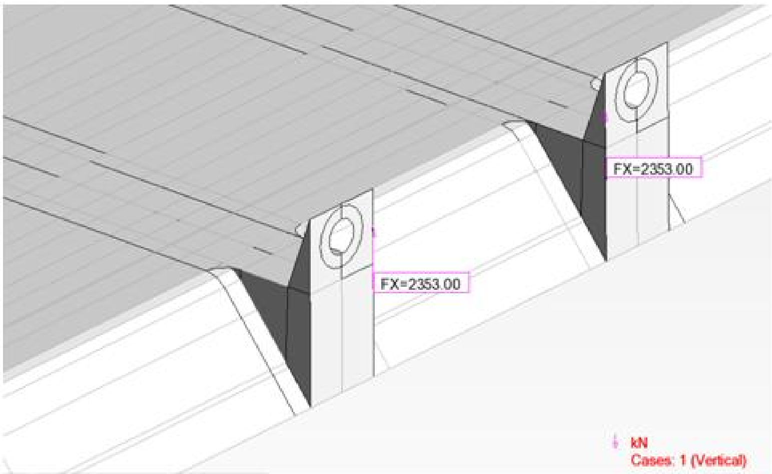

Figure 6-5 Applied reaction from the sheave block

The von Mises stresses for this load case is shown in Figure 6-6.

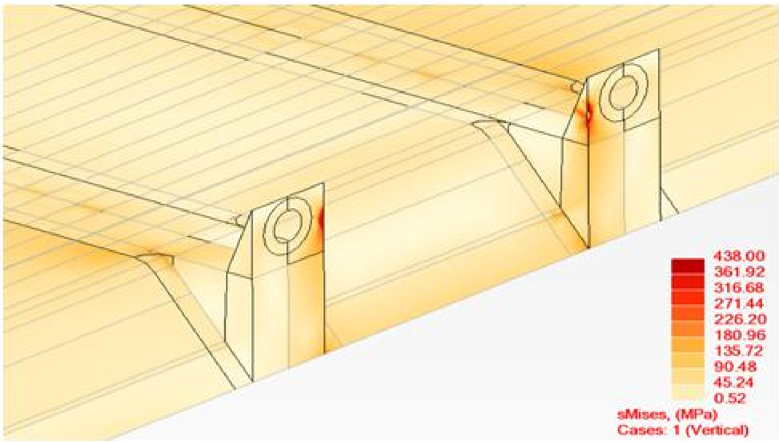

Figure 6-6 Von Mises stresses for the applied reaction from the sheave block

The steel quality of all hanger anchorages and cross girders are S460 and as shown in Figure 6-6 the maximum stresses is below f_{yd} = 460/γ_{M0} = 438MPa whereas the stress level during lifting of the general deck element in the hanger anchorage is verified.

There have been raised an alternative erection method shown on Cimolai drawing 2002159D0002550 dated 04-12-2010. With reference to Figure 6-7 the present design of the hanger anchorage the vertical reaction from the hanger is transferred directly from the anchor plate to the cross girder web plate. With this alternative erection method the vertical hanger reaction will during erection be transferred to the adjacent longitudinal steel through a bolted connection.

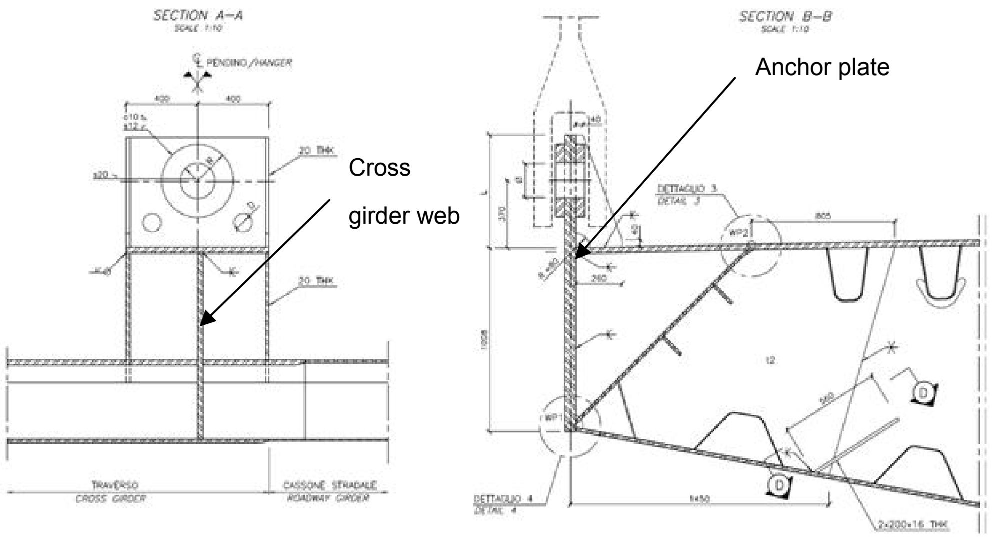

Figure 6-7 Present design of the hanger anchorage

To transfer the vertical hanger reaction from the anchor plate to the adjacent longitudinal steel and further to the cross girder web will require a relatively high degree of reinforcement of the existing design.

7 Local load effects - extension truss

The maximum vertical reaction from the extension truss acting on the roadway girder is at the position shown in Figure 7-1. The vertical reaction from the multi wheeler closest to the free edge of the girder at this truss position is according to Cimolai drawing no. 2002159D0002540 stated to be two times 95t per cantilevered girder.

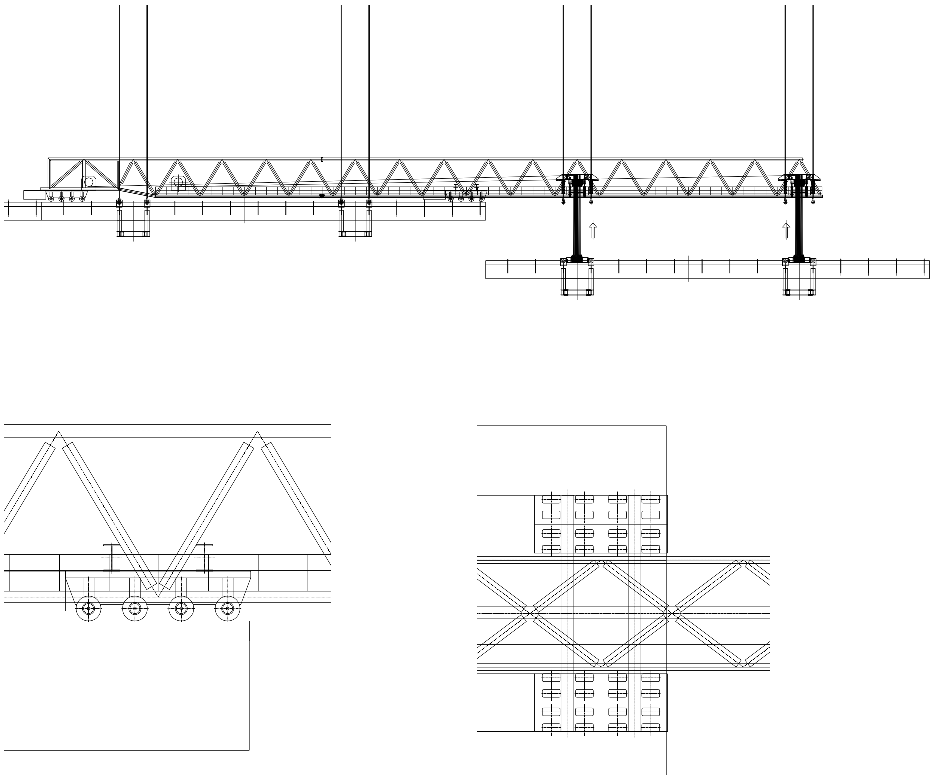

Figure 7-1 Elevation showing the lifting sequence and close-up of multi wheeler acting on the roadway girder

With sixteen wheels per multi wheeler and a safety factor of 1.35 the design stress reaction under a 400x400mm patch load acting on the roadway girder is:

$$\sigma_{\text{patch load,d}} = \frac{95000 \cdot 9.81 \cdot 1.35}{16 \cdot 400 \cdot 400} = 0.492\text{MPa}$$

This load is applied on the local FE-model of the CS1 roadway girder as shown in Figure 7-2 and Figure 7-3. The length of the cantilevered part of the girder from cross girder web to free edge has been modelled. The cantilevered part has the length x=17.275m. The FE-model has been modelled with a fixed support at the connection to the cross girder.

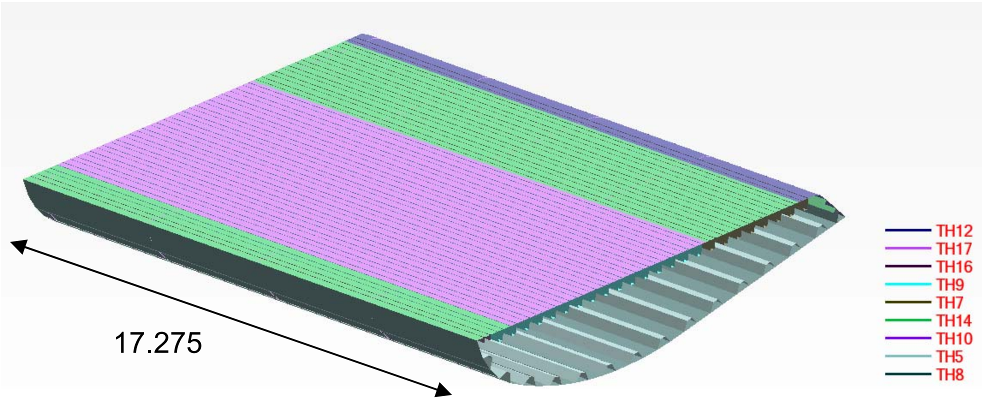

Figure 7-2 Plot of local shell model showing plate thicknesses

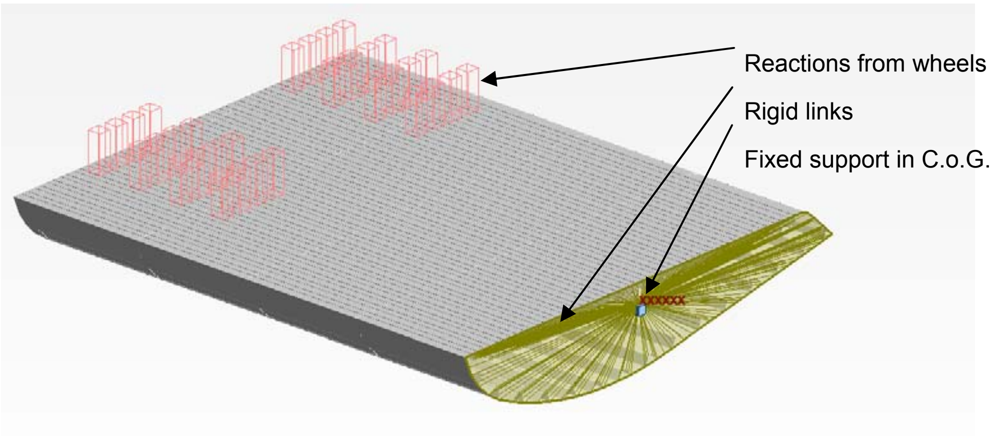

Figure 7-3 Plot of the local model showing applied wheel patch loads and supports

The ULS combination for this verification is 1.35 x PP and 1.35 x wheel load. The dead load is directly generated volumetric load from the shell elements in the FEM-model and the super imposed dead load is included as 10% of the volumetric load. The von Mises stresses for the design wheel patch load is shown in Figure 7-4.

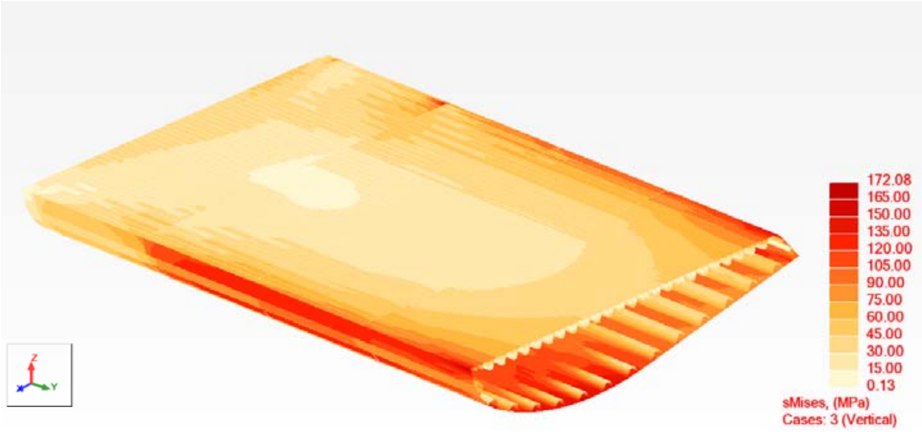

Figure 7-4 Von Mises stresses for design wheel load applied as patch load

As shown in Figure 7-4 the maximum design von Mises stress from the applied wheel load is 172MPa which is relatively close to the 189MPa found by Cimolai in the calculation note "Roadway segments during assembly phases". The von Mises stresses for the ULS combination with the dead load is shown in Figure 7-5.

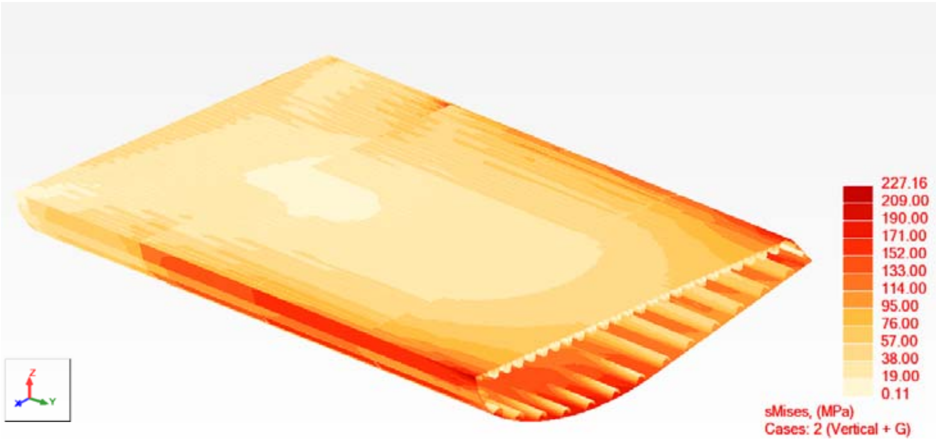

Figure 7-5 Von Mises stresses for load combination with combined dead and wheel load

The maximum von Mises stress in the load combination is 227MPa. The steel quality for the CS1 roadway section is S355 and the maximum stress is $f_{yd} = 355/\gamma_{M0}$ = 338MPa which is higher than the maximum von Mises stress.

This stress verification is a linear verification, but from the overall verification made for the roadway deck the considered section is stated as section class 4. Thus effective cross section properties need to be used for the verification, which seems not to have been used in the calculations by

Cimolai. The purpose made spread sheet ADVERS is used for verification of the section at the fixed support, located as shown in Figure 7-3. The reaction for the design load combination in the fixed support is shown in Table 7-1.

Table 7-1 Reactions in the fixed support for ULS combination

Node/Case	FX (kN)	FY (kN)	FZ (kN)	MX (kNm)	MY (kNm)	MZ (kNm)
957/ 2 (C)	-0.00	0.00	3456.47	-39545.32	1919.72	1.85

The corresponding von Mises stresses is found for the effective section in the stress points shown in Figure 7-6.

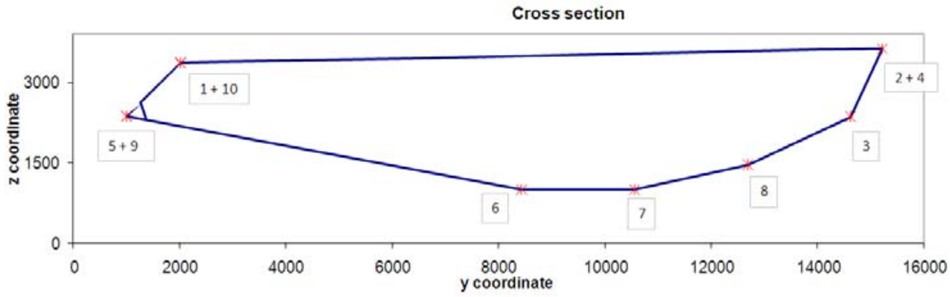

Figure 7-6 Stress points for the roadway section in ADVERS

The relating von Mises stresses and utilisation ratios in these stress points are shown in Table 7-2.

Table 7-2 Reactions in the fixed support for ULS combination

Plates - summary of governing check

ID	Yielding of plates						
	Criteria (gov.)	σ_1 (MPa)	σ_2 (MPa)	τ (MPa)	σ_{VM} (MPa)	σ_{yf}/γ_m (MPa)	UR
SP1	min NS	75.67		73.5	148.1	338.1	0.44
SP2	min NS	63.15		73.1	141.4	338.1	0.42
SP3	min NS	-119.17		75.0	176.3	338.1	0.52
SP4	min NS	64.43		75.0	145.0	338.1	0.43
SP5	min NS	-64.81		75.0	145.1	338.1	0.43
SP6	min NS	-294.13		75.0	321.5	338.1	0.95
SP7	min NS	-302.32		75.0	329.0	338.1	0.97
SP8	min NS	-242.89		75.0	275.4	338.1	0.81
SP9	min NS	-66.02		73.5	143.4	338.1	0.42
SP10	min NS	75.91		73.5	148.2	338.1	0.44
Max							0.97

As shown in Table 7-2 the maximum stresses utilisation in the effective section is 0.97. Since this relatively high stress utilisation of 0.97, located in the bottom plate, is due to compression forces the buckling of the stiffeners and plates has also to be verified.

Figure 7-7 shows the location of stress points at the critical troughs indicated as "SP-U_Stiff." in conjunction with the bottom plate from roadway section in ADVERS.

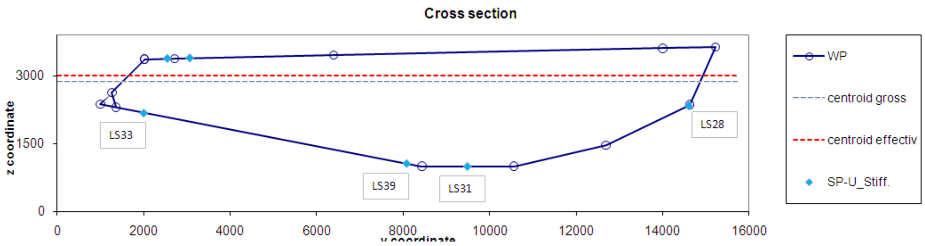

Figure 7-7 Numbering of the stress points for troughs from the roadway section in ADVERS

The utilisation ratios for buckling of stiffeners and plate are shown in Table 7-3.

Table 7-3 Utilisation ratios for buckling of stiffeners and panels.

ID	Buckling of Stiffener/Panels			(U-stiffeners)	
	Criteria	σ_1	σcr	Local	UR
	(gov.)	(MPa)	(MPa)	Traffic	(MPa)
LS28	min NS	-67.57	184.4	n	0.37
LS31	min NS	-187.70	184.4	n	1.02
LS33	min NS	-50.26	184.4	n	0.27
LS39	min NS	-177.52	186.8	n	0.95
Max					1.02

As shown in Table 7-3 the stiffener LS31 is over utilised by 2.0% in buckling check for the ULS load combination. The calculations show that the cross section is utilised to the very limit, however this may still be ok during the short erection period.

8 Local load effects - erected deck near tower

This section includes an assessment of the local load effects on de deck section near the tower. It should be noted that the procedure has been subsequently modified, and the main force is transferred directly to the transverse beam, avoiding over stresses in deck.

The lift of girder segments near the tower is carried out partly from the tower and partly from the two cantilevered roadway decks in segment 26C as shown in Figure 8-1.

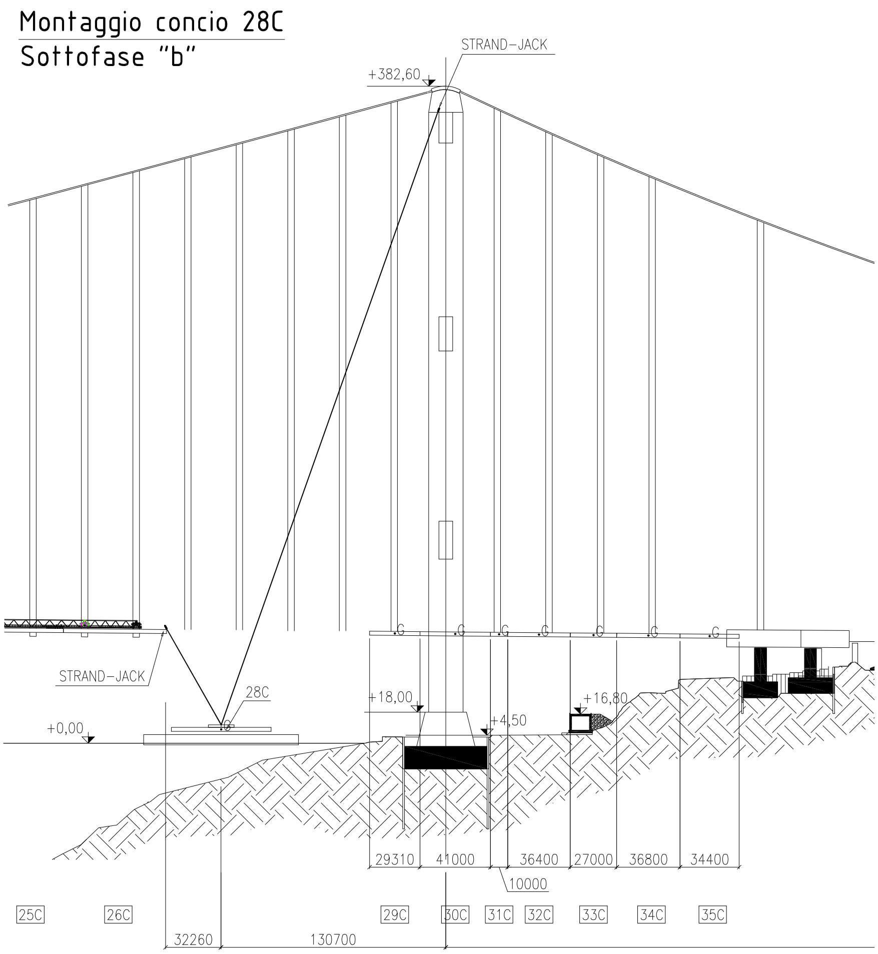

Figure 8-1 Erection phase of segment 28C

For the cantilevered roadway deck segment 26C the critical lift is the lift of segment 28C which is the heaviest of the eight segments installed with this procedure.

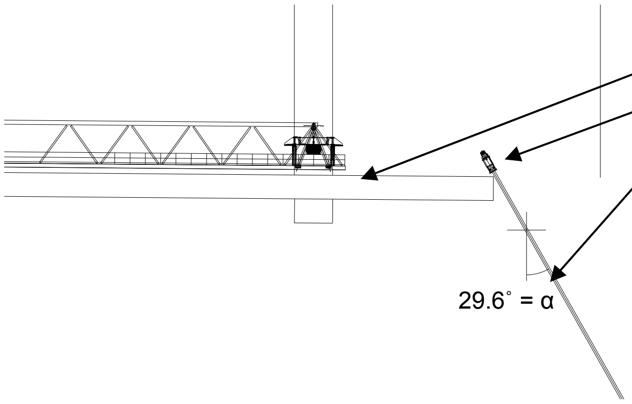

Figure 8-2 Close up of the initial lifting of 28C at segment 26C

As shown in Figure 8-2 the initial lifting angle at each of the two cantilevered roadway girders is 29.6˚. The weight of segment 28C is shown in Table 8-1.

Table 8-1 Weight of erection segment 28C

Element	**Dead load [kN/m]**	**Nos. / Length [m]**	**Total [kN]**
Cross girder T1	1580	1	1580
Cross girder T3	2000	1	2000
Roadway girder CS5	50.4	27.6	1391
Roadway girder CS3	43.0	73.5	3161
Railway girder CF3	38.5	13.8	531
Railway girder CF5	30.8	36.8	1133
Hanger anchorage AP4	35.2	8	282
Service lane, without wind screen, base plates and additional weight under transportation.			1008
Grand Total			11086

As shown in Figure 8-1 the distance from the tower to the segment is 130.7m and the distance from the tower to the strand jack at segment 26C is 163.0m.

The vertical lifting component at each of the two roadway girders is found with an estimated dynamic factor of 1.10, 1.25 for skewing effect for a lift with four lifting points and a safety factor of 1.35 as:

$$\mathrm{R}_{26\mathrm{C,v,d}} = \frac{130.7 \cdot 1.1 \cdot 1.25 \cdot 1.35 \cdot 11086}{163 \cdot 2} = 8250\mathrm{kN}$$

The horizontal lifting component at each of the two roadway girders is found as:

$$\mathrm{R}_{26\mathrm{C,H,d}} = \tan(29.6) \cdot 8250 = 4687\mathrm{kN}$$

The cantilevered cross section in segment 26C is roadway section CS3. A local FE-model of the CS3 cross section is shown in Figure 8-3.

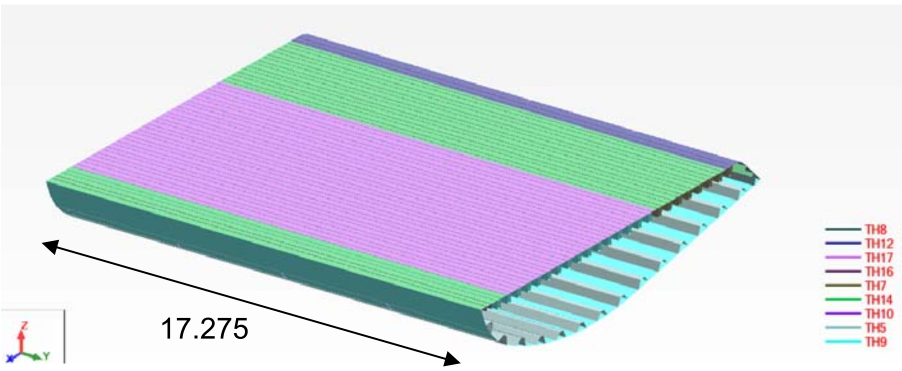

Figure 8-3 Plot of local shell model showing plate thicknesses

The vertical and horizontal initial design reaction at the 26C segment is applied to the local FE-model as shown in Figure 8-4. According to the geometry shown in Figure 8-2 the load is applied in a fictive point 1070mm above the top flange at the diaphragm and in line with the centre of gravity of the roadway girder. The load at this fictive point is connected by a rigid link to two 2600mm transverse lines at the two diaphragms with 3750mm distance. This rigid link represents a structure capable of distributing the reaction from the strand jack to these two support lines.

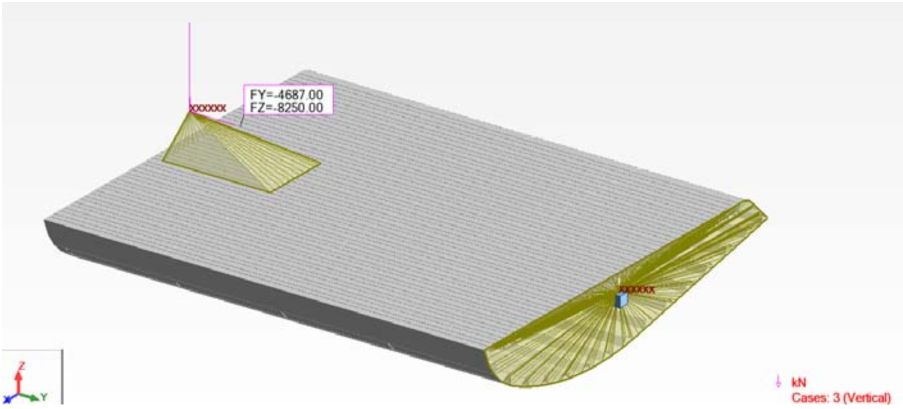

Figure 8-4 Plot of the local model showing applied wheel patch loads and supports

The von Mises stresses are shown in Figure 8-5 for a load combination of 1.35 x PP including 10% superimposed dead load and 1.35 x the characteristic lifting components.

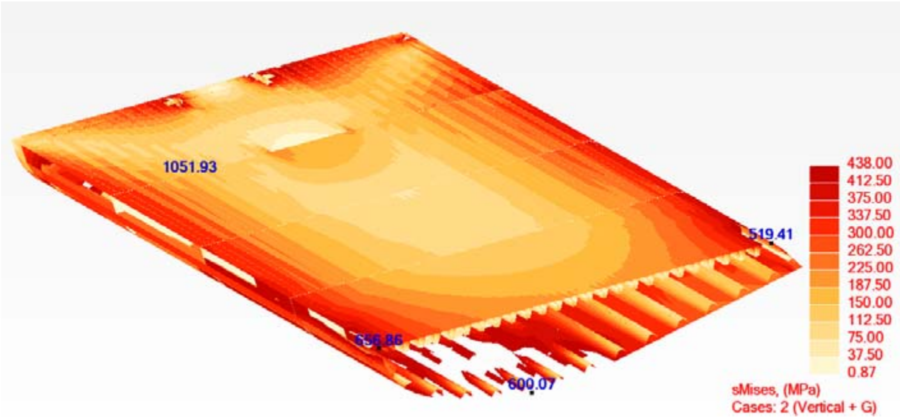

Figure 8-5 Von Mises stresses for load combination with combined dead and

The steel quality for the CS3 roadway section is S460 and the maximum stress is $f_{yd} = 460/\gamma_{M0} = 438$MPa. The stress scale in Figure 8-5 is limited to the f_{yd} whereas the yielding areas are shown as transparent areas.

As shown in Figure 8-5 the stress level from this linear model is much to high, whereas there must be found an alternative support position for the strand jack or strengthen the cantilevered part of the roadway deck. Due to the stresses in Figure 8-5 there is no reason for making any buckling check for this section. The proposed method has to be revised.

9 Local effects during storage and transportation of deck elements

The transport situation of deck elements according to Cimolai drawing 2002159D0006500 is shown in Figure 9-1 and Figure 9-2.

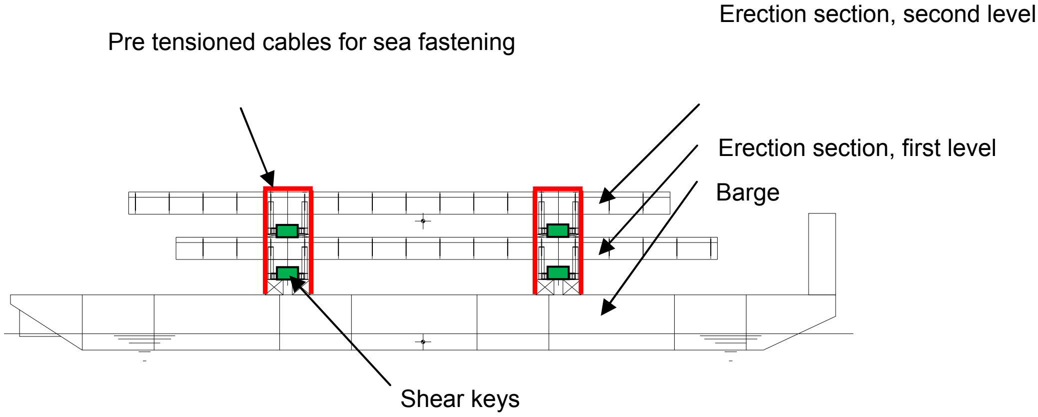

Figure 9-1 Elevation of barge with sea fastening of erection segments

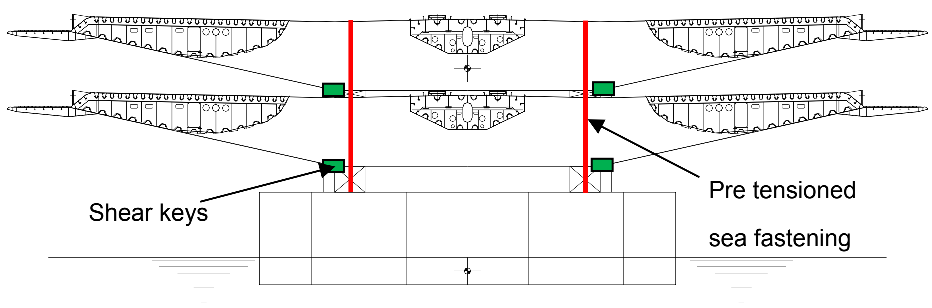

Figure 9-2 Section in barge with sea fastening of erection segments

ULS design loads are determined according to estimated accelerations during transportation, shown in Table 9-1.

Table 9-1 Estimated motion accelerations

Motion	Description	
Roll	Amplitude: α = 20˚ (deg)	Period Tα = 10s
Pitch	Amplitude: β = 12.5˚ (deg)	Period Tβ = 10s
Heave	Acceleration amplitude: γ = 0.2g	

The estimated motion accelerations shown in Table 9-1 results in a maximum vertical ULS-reaction from the first level at 7.5MN per. 400x400mm support at each side of the cross girder. The design stress reaction acting on the bottom of the cross girder becomes:

$$\sigma_{\text{patch load,first level,d}} = \frac{7.5 \cdot 10^6}{400 \cdot 400} = 46.9\text{MPa}$$

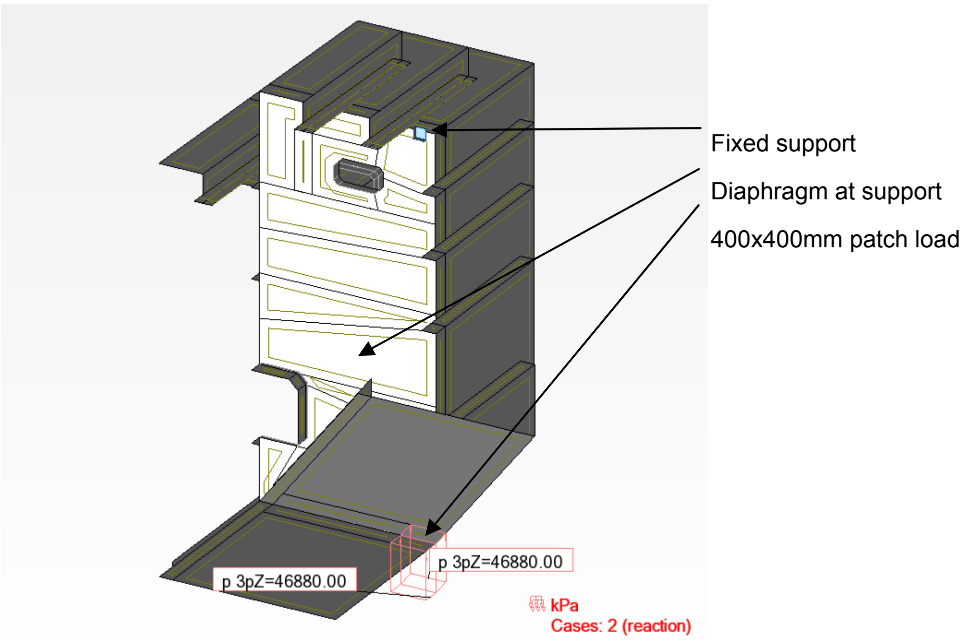

Figure 9-3 General cross girder seen from below with support reaction at first level

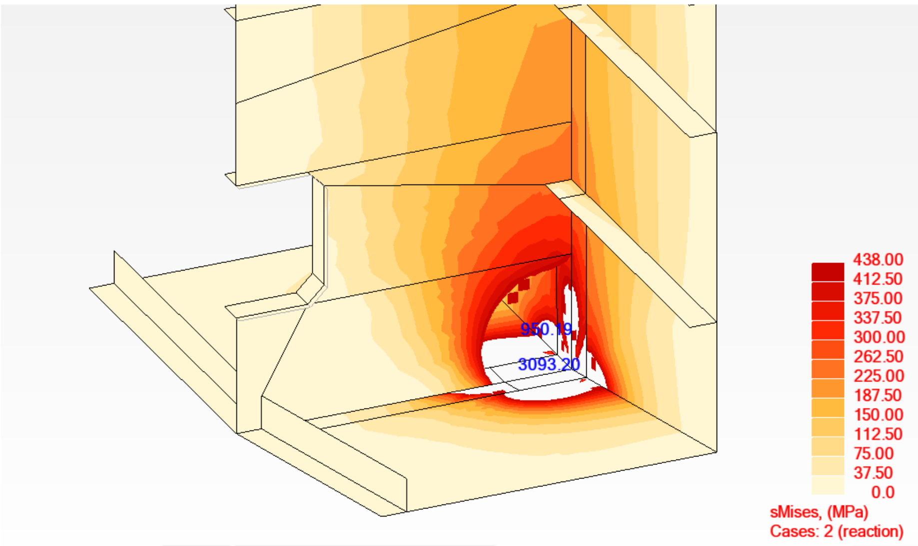

Figure 9-4 Von Mises stresses in diaphragm in general cross girder with support reaction at first level

As shown in Figure 9-4 the maximum von Mises stresses locally exceeds $f_{yd} = 460/\gamma_{M0} = 438$MPa whereas the proposed method has to be optimized in next project stage.

10 References

/1/ FHWA, State-of-the-art methods for calculating flutter, vortex-induced, and buffeting response of bridge structures, Report nr. FHWA/RD-80/050, April 1981.

/2/ FORCE Technology. Sub-test 4 Section Model Tests for the Messina Strait Bridge. Report no. 110-26444, Rev. A, December 2010.